# Coherence in the B800 Ring of Purple Bacteria LH2

Y. C. Cheng and R. J. Silbey

*Department of Chemistry and Center for Materials Science and Engineering, Massachusetts Institute of Technology, Cambridge, Massachusetts 02139, USA*

(Received 17 August 2005; published 17 January 2006)

We study the quantum coherence in the B800 ring and how it affects the dynamics of excitation energy transfer (EET) in photo-synthetic light-harvesting systems. From an analysis of the spectrum, we determine the disorder parameters for the B800 ring and show that the relatively weak electronic coupling between B800 pigments subtly changes the dynamics of EET and improves the uniformity and robustness of B800 $\rightarrow$ B850 EET at room temperature, an example of how a multichromophoric assembly can exploit coherence to optimize the efficiency of photosynthesis. A molecular-level description for the dynamics of EET in the light-harvesting system may prove useful for understanding other nanoscale molecular assemblies and designing efficient nanoscale optical devices.

DOI: 10.1103/PhysRevLett.96.028103 PACS numbers: 87.15.Mi, 71.35.−y, 73.22.−f, 85.60.Bt

The optical properties of nanoscale molecular aggregates have drawn considerable attention both experimentally and theoretically due to their important role in biological processes and synthetic molecular devices. One of the most studied molecular assemblies is the photosynthetic unit of purple bacteria [1–3], in which light-harvesting antenna systems capture solar energy and transfer the excitation energy to the reaction center to drive the photo-synthetic reaction. These light-harvesting complexes store and transfer excitation energy with astonishingly high efficiency (above 95%); thus, understanding the underlying design principles of photo-synthetic light-harvesting systems can lead to improvements of the design of synthetic antenna devices.

The high-resolution x-ray structures of the LH2 complexes of purple bacteria revealed remarkable symmetry in the arrangement of bacteriochlorophylls (BChls) in the pigment-protein complexes and have motivated extensive studies on those systems [4,5]. For example, the LH2 complex of *Rhodopseudomonas acidophila (Rps.)* carries 27 BChl *a* molecules in two concentric rings embedded in the surrounding proteins; 9 of the BChl molecules form the B800 ring which absorbs maximally at 800 nm, and the other 18 form the B850 ring which absorbs maximally at 850 nm. The entire complex has ninefold symmetry. The BChl molecules in the B850 ring are closely packed, which leads to strong electronic coupling of $\sim$300 $\mathrm{cm}^{-1}$ between adjacent pigments [6]. In contrast, the large distance between adjacent BChl molecules results in weak nearest-neighbor couplings ( $\sim -27$ $\mathrm{cm}^{-1}$) in the B800 ring [7,8].

In order to understand the nature of excitations and dynamics of excitation energy transfer (EET) in the LH2 complexes of purple bacteria, a molecular-level description is essential. Spectroscopic studies, especially recent single-molecule (SM) experiments, have significantly advanced our knowledge about these processes; however, a detailed understanding is still not at hand, mainly due to the difficulty of characterizing the quasistatic disorder due to the slow fluctuations of local protein environments and pigment structures in LH2. These fluctuations can lead to disorder in the excitation energies of the BChl molecules in a single LH2 complex (intracomplex energy disorder). In addition, both ensemble [9] and SM [10] spectroscopy show that there is also intercomplex disorder that changes the average excitation energy in each LH2 complexes. It has been clearly established that quantum coherence in the B850 ring of LH2 plays a crucial role in light-energy harvesting, storage, and transfer [11–13]. Because the electronic coupling between B850 BChls is sufficiently large [1,3,14], a delocalized Frenkel exciton description is required for B850 excited states. In contrast, for the B800 ring, excitations are usually considered to be localized on individual pigments because the couplings between B800 BChls are smaller than the energetic inhomogeneities in the system [9,10]. Although SM studies using polarization-dependent spectroscopic techniques have provided strong evidence that excitations in the B800 band are delocalized on two or three pigments [15,16], the effect of the B800 coherence is usually not considered. In this Letter, we focus on the B800 ring of *Rps.* and demonstrate that, contrary to conventional wisdom, quantum coherence in the B800 ring cannot be neglected. We show that the type and degree of disorder in the B800 ring can be extracted from the ensemble spectrum, and that the effect of coherence in the B800 ring subtly changes both the spectrum and EET dynamics in the LH2.

We consider a single system of $N$ pigments in a circular geometry described by the exciton Hamiltonian

$$H = \sum_{n=1}^{N} E_n |n\rangle\langle n| + \sum_{n \neq m} J_{nm} |n\rangle\langle m|, \qquad (1)$$

where $|n\rangle$ denotes a $Q_y$ excited state localized at site $n$, $E_n$ is the excitation energy of $|n\rangle$, and $J_{nm}$ is the electronic coupling between $|n\rangle$ and $|m\rangle$. For the B800 ring, the couplings between the next-nearest-neighbor pigments are weak; therefore, we consider only the nearest-neighbor

 

couplings $J_{n,n\pm1}$. To consider static disorder, we treat $E_n$ and $J_{n,n+1}$ as having random components: $E_n = E(0) + \delta E_I + \delta E_D(n)$ and $J_{n,n+1} = J(0) + \delta J(n)$, where $E(0)$ and $J(0)$ are ensemble average values, $\delta E_I$ is the intercomplex energy disorder for the ring, $\delta E_D(n)$ is the intracomplex energy disorder (diagonal disorder) at site $n$, and $\delta J(n)$ is the disorder in the nearest-neighbor coupling (off-diagonal disorder). We assume $\delta E_I$, $\delta E_D(n)$, and $\delta J(n)$ are independent Gaussian random variables with zero mean and standard deviations $\sigma_I$, $\sigma_D$, and $\sigma_J$, respectively. Given $\sigma_I$, $\sigma_D$, and $\sigma_J$, we numerically generate and diagonalize $H$ to obtain eigenstates, $H|\phi_\alpha\rangle = \varepsilon_\alpha|\phi_\alpha\rangle$, where $\varepsilon_\alpha$ is the excitation energy of the $\alpha$th exciton state, and the eigenfunction $|\phi_\alpha\rangle = \sum_n c_n^\alpha|n\rangle$. If the transition-dipole moment of $|n\rangle$ is denoted as $\vec{\mu}_n$, the transition-dipole moment of $|\phi_\alpha\rangle$ can be written as $\vec{M}_\alpha = \sum_n c_n^\alpha \vec{\mu}_n$. The ensemble spectral line shape can then be represented as $I(\omega) = \langle \sum_\alpha |\vec{M}_\alpha|^2 \delta(\omega - \varepsilon_\alpha)\rangle_s$, where the bracket $\langle \ldots \rangle_s$ represents the ensemble average over static disorder. To compute $I(\omega)$, Monte Carlo simulations are carried out using 100 000 realizations of disordered $H$. Note that we only consider static disorder at this stage; electron-phonon coupling and other dynamical effects are neglected. Because the B800 BChls are weakly coupled to phonon modes and the observed homogeneous linewidth is much smaller than the inhomogeneities in the B800 band, at low temperatures static disorder dominates the line shape and dynamical effects are negligible [15,17].

We examine the B800 ring of *Rps.* for which $N = 9$ and $J(0) = -27$ cm$^{-1}$ [8]. In addition, we assume $|\vec{\mu}_n| = \mu_0$ with dipole orientations taken from the x-ray data [4]. Spectra with a broad range of $\sigma_I$, $\sigma_D$, and $\sigma_J$ are simulated and compared to a low-temperature ensemble spectrum from the Köhler group [18]. We find reasonable fits located at $\sigma_I = 10 \pm 5$ cm$^{-1}$, $\sigma_D = 60 \pm 10$ cm$^{-1}$, and $\sigma_J = 15 \pm 5$ cm$^{-1}$. Our fit also indicates that the off-diagonal disorder *cannot* be ignored. In addition, our estimate of $\sigma_D$ is in excellent agreement with SM experiments [10], providing an independent confirmation to the interpretation of the SM experiments, and demonstrating the possibility of extracting the degree of disorder and coherence from ensemble measurements.

Figure 1(a) shows the simulated density of states and spectral line shape for an ensemble of B800 rings with $\sigma_I = 10$ cm$^{-1}$, $\sigma_D = 60$ cm$^{-1}$, and $\sigma_J = 15$ cm$^{-1}$. While the density of states is a symmetric function, the spectral line shape is asymmetric. The maximum of the line shape is redshifted from the average energy, and a pronounced tail in the blue side of the band can be clearly seen. We also compare the simulated spectrum to the low-temperature ensemble spectrum. The excellent agreement indicates that although the B800 line shape is dominated by inhomogeneous line broadening, as expected, the effect of coherence exists and results in the blue tail. Since the absorption spectrum is modeled as the density of states weighted by the dipole strength $|\vec{M}_\alpha|^2$, the asymmetric line

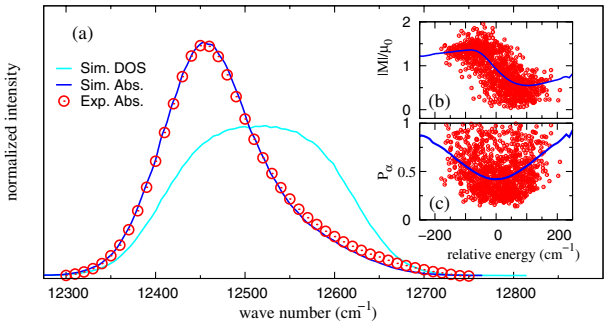


FIG. 1 (color online). Results for $\sigma_I = 10$ cm$^{-1}$, $\sigma_D = 60$ cm$^{-1}$, and $\sigma_J = 15$ cm$^{-1}$. (a) The simulated density of states and spectral line shape. The open circle denotes the experimental spectrum. (b) Scatter plot of normalized dipole moment and (c) participation ratio for exciton states of 100 realizations of B800 rings. The solid lines are average values.

shape indicates an asymmetric distribution in dipole strengths. Figure 1(b) shows the distribution of dipole moments as a function of the relative B800 excitation energy. The distribution exhibits an anticorrelated behavior; the states in the red side of the band have stronger dipole strengths than those in the blue side. The redistribution of dipole moments indicates that the excitations are coherently delocalized to some extent. In Fig. 1(c), we show the distribution of the participation ratio $P_\alpha = \sum_n |c_n^\alpha|^4$ [20] for the B800 excitations. Note that the inverse of $P_\alpha$ is a measure of the delocalization length. The average participation ratio ranges from 0.4 in the center to about 0.9 in both edges of the band, indicating that exciton states at the edges of the band are more localized, as expected. A majority of the states have participation ratio in a range from 0.25 to 0.6, corresponding to delocalized excitons on 2–4 pigments. For the set of disorder parameters that reproduces the low-temperature ensemble spectrum of the B800 ring of *Rps.*, our calculation clearly shows that the coherence in the B800 ring cannot be neglected, and the blue tail in the ensemble spectrum is actually a signature of the quantum coherence. A pronounced blue tail is also observed in the B800 absorption spectrum at room $T$, suggesting that the dynamical localization effects at higher temperatures do not fully destroy the coherence in the B800 ring. In addition, Matsuzaki *et al.* [21] studied an LH2 complex of *Rps.* containing only one $BChl_{800}$ molecule, with no possible coherence. The spectrum of this B800-deficient sample shows a more Gaussian-like profile, supporting our interpretation of the effect of coherence.

Since the average participation ratio is close to 0.5 in a broad range of the B800 band, a reasonable zeroth-order description for the B800 excited states is a coherent excitation delocalized on nearest-neighbor dimers. We have simulated the B800 spectrum using a dimer Hamiltonian with diagonal and off-diagonal static disorder, and the result successfully captures the important spectral signatures. In the following, we will apply the dimer picture to

examine the effect of B800 coherence on the dynamics of B800 intraband and B800 → B850 interband EET.

*Dynamics of B800 intraband transfer.*—Spectroscopic experiments have identified a fast decay channel with wavelength dependent rates in the blue side of the B800 band [10,22–24]. This extra decay channel has been attributed to B800 intraband EET [24,25], and its dynamics has been described either as incoherent hopping of excitations between monomers [9,25] or coherent relaxation in the exciton manifold [10]. However, so far no theoretical model can quantitatively explain the wavelength dependent rates. We apply a simplified dimer exciton bath to describe the B800 intraband transfer. Based on Eq. (1), we use an effective disordered dimer Hamiltonian $H_0 = E_1|1\rangle\langle 1| + E_2|2\rangle\langle 2| + J(|1\rangle\langle 2| + |2\rangle\langle 1|)$, with an upper and a lower dimer exciton state located at $E_\pm = (E_1 + E_2)/2 \pm \sqrt{(E_1 - E_2)^2/4 + J^2}$. The total Hamiltonian is $H = H_0 + H_b + V$, where we consider independent harmonic baths $H_b = \sum_n \omega_n (b_n^\dagger b_n + 1/2)$ and a general linear electron-phonon ($e$-ph) coupling term $V = B_1|1\rangle\langle 1| + B_2|2\rangle\langle 2|) + B_j(|1\rangle\langle 2| + |2\rangle\langle 1|)$, with $B_\alpha = \sum_n g_{n\alpha}(b_n^\dagger + b_n)$ for $\alpha = 1, 2, j$. Assuming that $B_1$, $B_2$, and $B_j$ are not correlated and the $e$-ph couplings are weak, we derive the downward relaxation rates $\Gamma_d$ and $\Gamma_j$ using Fermi's golden rule, where $\Gamma_d$ and $\Gamma_j$ are relaxation rates due to diagonal ($B_1$ and $B_2$) and off-diagonal ($B_j$) $e$-ph couplings, respectively. We calculate the functions $C_\alpha(t) = \langle B_\alpha(t) B_\alpha(0)\rangle_{\rm eq}$ from a spectral function that fits the BChl molecular spectrum [19], $\sum_n g_{n\alpha}^2 \delta(\omega - \omega_n) = \gamma_\alpha(0.5\omega + 0.58\omega^2/\omega_c)e^{-\omega/\omega_c}$, where $\gamma_\alpha$ represents relative $e$-ph coupling strengths and $\omega_c = 100\ {\rm cm}^{-1}$ is the cutoff frequency. We assume the lifetimes and homogeneous linewidths of B800 excited states are determined exclusively by the B800 downward relaxation and B800 → B850 EET. At low temperatures, the linewidths of the upper and lower levels are $\Gamma_U = \Gamma_0 + \Gamma_d + \Gamma_j$ and $\Gamma_L = \Gamma_0$, respectively, where we have assumed a constant B800 → B850 rate $\Gamma_0$. Using the same disorder parameters as before and $\Gamma_0 = 1.7\ {\rm cm}^{-1}$, we calculate the average linewidth across the B800 band at $T = 0$ K as a function of relative spectral position. In Fig. 2, we show two theoretical curves, one with only diagonal $e$-ph coupling ($\Gamma_d$-only) and the other with only off-diagonal $e$-ph coupling ($\Gamma_j$-only), and compare them with the homogeneous linewidths measured in low-temperature SM experiments [10]. For the $\Gamma_j$-only case, we use $\gamma_j = 0.04$ to obtain the best fit to the experiment. For the $\Gamma_d$-only case, $\gamma_1 = \gamma_2 = 0.1$ is used. Both models give reasonable $e$-ph coupling strengths and are in qualitative agreement with experiment. Note that the $\Gamma_j$-only model describes the wavelength dependence and the activation of the relaxation channel semiquantitatively, and is also consistent with hole-burning experiments [22,25]. Our result suggests that B800 intraband EET is due to phonon induced relaxation in the exciton manifold, and that the phonon induced fluctuations

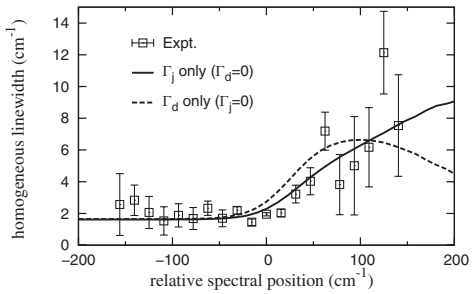


FIG. 2. Comparison of the theoretical homogeneous linewidth with the single-molecule measurements in Ref. [10]. The relative spectral position is the position of the absorption lines with respect to the spectral mean of a single B800 ring.

in $J$ play a major role in the process. Note that our model includes hopping between nearest-neighbor sites in the $E \gg J$ limit.

*Dynamics of* B800 → B850 *transfer.*—Much effort has been focused on the calculation of the B800 → B850 EET rate within a single LH2 [11–13]. However, while the coherence in the B850 ring has been proved to be crucial for the efficient B800 → B850 EET, the B800 coherence was generally neglected. To study the effect of the B800 coherence, we consider theoretical B800 → B850 rates for two simplified models for the B800 ring: a B800 BChl monomer, and a B800 BChl dimer that includes the coherence between nearest-neighbor pigments [26]. We assume the B850 effective Hamiltonian in Ref. [6] and the $e$-ph coupling in Ref. [19], and the interactions between B800 and B850 BChls in Ref. [8] are employed. We also consider energetic disorder that reproduces the ensemble spectrum of the LH2 from *Rps.* [27]. B800 → B850 EET times at $k_BT = 10\ {\rm cm}^{-1}$ are calculated using the multichromophoric Förster resonance energy transfer (MC-FRET) theory [13] for the monomer model ($\tau_M$), and for both the lower levels ($\tau_L$) and upper levels ($\tau_U$) of the dimer model. Figure 3(a) shows the distributions of the theoretical B800 → B850 EET times. The ensemble average values of $\tau_M$, $\tau_L$, and $\tau_U$ are 1.3 ps, 1.6 ps, and 1.2 ps, respectively. At low temperatures, the equilibrium B800 → B850 rate is given by $\tau_L$. The theoretical value of 1.6 ps is in agreement with experimental transfer time of 1.6 ± 0.2 ps

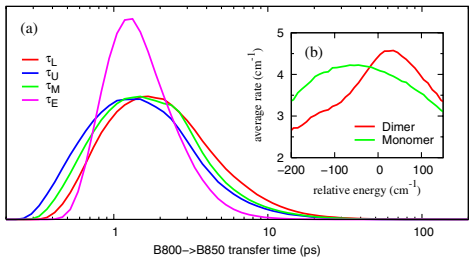


FIG. 3 (color online). (a) The distribution of the theoretical B800 → B850 EET times at $k_BT = 10\ {\rm cm}^{-1}$. (b) The average B800 → B850 rate as a function of the energy relative to the average B800 excitation energy.

determined by femtosecond pump-probe spectroscopy [23]. In Fig. 3(b), we show the average rate as a function of the B800 excitation energy for both models. The monomer model gives a relatively weak energy dependence for the B800 → B850 EET rate, a result that is consistent with the measurement made on B800-deficient LH2 [21]. The dimer model, however, gives a more dramatic energy dependence for the B800 → B850 EET rate; the rate is higher in the blue side of the band and lower in the red side of the band, contrary to the prediction of simple Förster theory, which would give faster rate for states in the red side of the band because of their stronger dipole strengths [see Fig. 1(c)]. Note that with this B850 Hamiltonian, our calculations suggest that the B800 coherence reduces the B800 → B850 EET rate at low temperatures. At room temperature, however, the rapid B800 intraband EET allows the upper levels to dominate the B800 → B850 dynamics, because both upper and lower levels can now transfer energy to the B850 ring. Thus the efficient B800 intraband EET, due to the B800 coherence, assists the B800 → B850 EET at room temperature. To demonstrate the effect, we calculate the B800 → B850 EET time for the dimer model at high $T$, $\tau_E = 2\tau_L\tau_U/(\tau_L + \tau_U)$. In Fig. 3(a), the distribution of $\tau_E$ is significantly narrower then the distribution of $\tau_M$, indicating that the B800 coherence makes the B800 → B850 EET process more uniform and hence more robust. We have also performed similar calculations using other B850 model Hamiltonians, and found that while the values and profiles in Fig. 3 are sensitive to the electronic couplings between B850 BChls, the distribution of $\tau_E$ is narrow regardless of the B850 Hamiltonians used. Thus, the coherence in the B800 ring creates more uniform pathways for B800 → B850 EET, and increases the rate of EET at room temperature. Finally, we point out that compared to the SM measurements shown in Fig. 2, our theoretical result overestimates the B800 → B850 rate in the red side of the band by about a factor of 2. While this disagreement does not alter our conclusion about the B800 intraband EET because the absolute value is small compared to the B800 intraband EET rate, we believe it indicates that the B850 Hamiltonian needs improvement.

Our calculations suggest that (a) the B800 ensemble line shape in the purple bacterium *Rps.* can only be understood when coherent interactions are included; (b) the B800 intraband energy transfer is described by energy relaxation in the partially coherent exciton manifold; and (c) the B800 coherence significantly changes the dynamics of the B800 to B850 EET. Additional calculations on *Rhodospirillum molischianum* indicate that B800 coherence also plays a similar role in that structure.

The authors would like to thank Professor J. Köhler for sharing unpublished experimental results. This research was supported by the NSF.

[1] V. Sundstrom, T. Pullerits, and R. van Grondelle, J. Phys. Chem. B **103**, 2327 (1999).
[2] T. Renger, V. May, and O. Kuhn, Phys. Rep. **343**, 137 (2001).
[3] X. C. Hu, T. Ritz, A. Damjanovic, F. Autenrieth, and K. Schulten, Q. Rev. Biophys. **35**, 1 (2002).
[4] G. McDemott *et al.*, Nature (London) **374**, 517 (1995).
[5] J. Koepke, X. C. Hu, C. Muenke, K. Schulten, and H. Michel, Structure **4**, 581 (1996).
[6] G. D. Scholes, I. R. Gould, R. J. Cogdell, and G. R. Fleming, J. Phys. Chem. B **103**, 2543 (1999).
[7] K. Sauer *et al.*, Photochem. Photobiol. **64**, 564 (1996).
[8] B. P. Krueger, G. D. Scholes, and G. R. Fleming, J. Phys. Chem. B **102**, 5378 (1998).
[9] R. Agarwal, M. Yang, Q. H. Xu, and G. R. Fleming, J. Phys. Chem. B **105**, 1887 (2001).
[10] A. M. van Oijen, M. Ketelaars, J. Kohler, T. J. Aartsma, and J. Schmidt, Biophys. J. **78**, 1570 (2000).
[11] K. Mukai, S. Abe, and H. Sumi, J. Phys. Chem. B **103**, 6096 (1999).
[12] G. D. Scholes and G. R. Fleming, J. Phys. Chem. B **104**, 1854 (2000).
[13] S. Jang, M. D. Newton, and R. J. Silbey, Phys. Rev. Lett. **92**, 218301 (2004).
[14] M. Ketelaars, A. M. van Oijen, M. Matsushita, J. Kohler, J. Schmidt, and T. J. Aartsma, Biophys. J. **80**, 1591 (2001).
[15] A. M. van Oijen, M. Ketelaars, J. Kohler, T. J. Aartsma, and J. Schmidt, Chem. Phys. **247**, 53 (1999).
[16] C. Hofmann *et al.*, Phys. Rev. Lett. **90**, 013004 (2003).
[17] C. Hofmann, H. Michel, M. van Heel, and J. Kohler, Phys. Rev. Lett. **94**, 195501 (2005).
[18] The B800-only spectrum is obtained by subtracting a simulated B850 spectrum from an LH2 absorption spectrum at 6 K. The B850 spectrum is generated using the line shape theory in Ref. [19]. To fit the B850 part, we chose Gaussian energy disorder and dipole orientation disorder with $\sigma$ equal to 220 $cm^{-1}$ and 10°, respectively.
[19] S. J. Jang and R. J. Silbey, J. Chem. Phys. **118**, 9324 (2003).
[20] D. J. Thouless, Phys. Rep. **13**, 93 (1974).
[21] S. Matsuzaki, V. Zazubovich, N. J. Fraser, R. J. Cogdell, and G. J. Small, J. Phys. Chem. B **105**, 7049 (2001).
[22] C. De Caro, R. W. Visschers, R. van Grondelle, and S. Volker, J. Phys. Chem. **98**, 10 584 (1994).
[23] H. M. Wu *et al.*, J. Phys. Chem. **100**, 12 022 (1996).
[24] J. M. Salverda, F. van Mourik, G. van der Zwan, and R. van Grondelle, J. Phys. Chem. B **104**, 11 395 (2000).
[25] V. Zazubovich, R. Jankowiak, and G. J. Small, J. Lumin. **98**, 123 (2002).
[26] The average excitation energy of $BChl_{800}$ is 515 $cm^{-1}$ higher than that of $BChl_{850}$, and the spectral function of Ref. [19] with $\gamma = 0.7$ is employed for $BChl_{800}$. For dimers, the nearest-neighbor coupling is $-27$ $cm^{-1}$.
[27] We employed Gaussian energetic disorder with the following standard deviations: 10 $cm^{-1}$ ($BChl_{800}$ intercomplex disorder); 65 $cm^{-1}$ ($BChl_{800}$ diagonal disorder); 50 $cm^{-1}$ ($BChl_{850}$ intercomplex disorder); 200 $cm^{-1}$ ($BChl_{850}$ diagonal disorder). More than 100 000 realizations of disorder are used for the ensemble average.